THE PERFORMANCE OF A CABLE-STAYED BRIDGE PYLON UNDER CLOSE-RANGE BLAST LOADS

S. Komeil Hashemi*, Mark A. Bradford and Hamid R. Valipour
Centre for Infrastructure Engineering and Safety,
School of Civil and Environmental Engineering, UNSW Australia,
UNSW Sydney, NSW 2052, Australia. *Email: s.hashemiheidari@unsw.edu.au

ABSTRACT

Recent bridge collapses have raised an awareness of, and a concern for, the safety and robustness of bridges subjected to blast loading scenarios. The incident pressure generated by the explosion can cause severe structural damage and a loss of critical structural members, resulting in partial collapse of the bridge. Previously, most relevant research effort has been devoted to understanding the response of buildings under blast loading and to develop guidelines to increase the resistance of such structures, while relatively little research attention has been focused on bridge structures. Recent advancements in numerical methods have enabled the viable and cost-effective simulation of complicated blast scenarios, and hence these methods provide a useful reference for safeguarding design and assessment of critical infrastructure. To reduce the computational costs, previous studies on long span bridges under blast loads typically take advantage of sub-structuring techniques, in which only part of the structure is modelled. However, such oversimplifications can lead to erroneous results. Accordingly, this study is an attempt to simulate the dynamic response of an entire cable-stayed bridge subjected to blast loading based on best practice techniques obtained from the literature. The response of a steel bridge, designed according to the minimum requirements of the Australian Standard AS5100, is investigated when subjected to blast loads ranging from small to large explosions at different positions above the deck using numerical simulations. In addition, the potential effects of blast loads on different structural components (*i.e.* the deck and pylons) are discussed and possible blast mitigation strategies such as the application of FRP and optimization of the geometry of the pylons are investigated.

KEYWORDS

Cable-Stayed, Bridge, Pylon, Numerical, Performance, Blast, LS-Dyna.

INTRODUCTION

Recent bridge collapses have raised an awareness of, and a concern for, the safety and robustness of bridges subjected to blast loading scenarios. The incident pressure generated by the explosion can cause severe structural damage and a loss of critical structural members, resulting in partial collapse of the bridge. The design provisions for blast resistant bridges are limited due to inadequate knowledge of the local and global dynamic response of the bridge components (i.e. piers, deck and cables) subjected to blast loading scenarios. Furthermore, the existing design guides for blast-resistant bridges are limited to particular structural components (NCHRP 2010).

Bridge structures are typically more vulnerable to extreme loading scenarios than buildings because bridges have less structural redundancy compared to buildings. Thus, in the case of failure of any primary structural members in bridges, redistribution of the applied load through an alternative load path to prevent potential progressive collapse is almost impossible. For example, failure of the pylon in cable-stayed bridges can cause complete collapse of the entire bridge. The loss of a critical bridge or tunnel can potentially lead to severe casualties and billions of dollars as direct reconstruction expenses. Furthermore, the socioeconomic costs involved in such a collapse can double the cost of constructing a new long span bridge (FHWA 2003).

To design bridges to withstand blast loads, an engineering understanding of blast wave propagation and its effects on structures is needed. Numerical techniques can be used to model the explosion and structure, so as to study the interaction between them. Recent advancements in numerical methods have enabled engineers to simulate complicated blast scenarios in a viable, efficient and cost-effective way and subsequently to provide useful reference data for the safeguarding design of critical infrastructures. Accordingly, computer simulations have been used by different researchers to capture the failure mode and dynamic response of cable stayed bridges subjected to hypothetical blast scenarios (Son and Lee 2011, Tang and Hao 2010, Hao and Tang 2010).

The finite element (FE) package MD Nastran was used by Son and Lee (2011) to evaluate the response of a hollow steel box pylon of a cable-stayed bridge subjected to blast loads. The interaction between the air blast and a part of cable stayed bridge pylon was captured by an Arbitrary Lagrangian Eulerian method (ALE). In Son and Lee's FE model, the cables were omitted and only the corresponding forces in the cables were applied on the model and assumed to be constant throughout the analysis. The FE predictions showed that the P-Δ effect can cause significant instability in the hollow steel box pylons subjected to a blast scenario. Using a concrete-filled steel section in the vulnerable part of the pylon demonstrated superior performance under blast loads.

Tang and Hao (2010) and Hao and Tang (2010) used the FE package LS-DYNA to study the numerical simulation of a fixed-base cable-stayed bridge under blast loading with damage prediction and possible retrofitting strategies. The simulation contained most important bridge components such as the pier, tower, back span and steel-concrete composite main span, but investigated individually. The failure of the bridge was predominantly due to compressive crushing and spalling of concrete materials with reinforcing bar and steel plate failure. The damage area of each bridge component was significant, but they are still localized, however this could cause bridge to lose its stability. Progressive collapse analysis of the bridge structure uncoupled with blast loading also showed failure of the main span was unlikely and back-span destruction did not extend through entire structure. Moreover the application of CFRP strengthening on the deck is ineffective even though strengthening does reduce the effects.

To reduce the computational costs, the previous studies typically take advantage of a sub-structuring technique, in which only part of the structure is modelled. However, such oversimplifications can lead to erroneous results. Hence, the dynamic response of an entire cable-stayed bridge with a truss deck subjected to blast was studied by Deng and Jin (2009) and it was concluded that the explosion can lead to localised destruction of the deck in the vicinity of the detonation. However, the dynamic response of the entire truss deck was insignificant, mainly because the truss elements were not affected by the air blast pressure.

It must be noted that the interaction between any structural components could affect the response of the entire structure in the event of blast explosion. Assessing the vulnerability of bridge individual elements cannot show the probable progressive collapse of entire bridge structure, while it is the first step to understand the extent of the damage. Designers also need to consider the post-blast behaviour of the damaged structure under gravity loads, and the instability it could cause. Consequently, it is of importance that the blast resistance of bridges, in particular those having a long span, be studied and necessary mitigation implemented for safety protection in the future. To this end, the current study intends to simulate the dynamic response of an entire steel cable-stayed bridge subjected to close-range detonation using the LS-DYNA (Hallquist 2014) explicit finite element package. The cable-stayed bridge was designed according to the minimum requirements of Australian standards (AS5100 2004) and analysed under dead, traffic and blast loads at different locations close to the pylon. The results of the FE models are used to assess the performance of bridge pylons and cables as well as the entire bridge exposed to an air blast.

Furthermore, the potential effects of blast loads on different structural components (*i.e.* deck and pylons) are discussed and values of the demand-to-capacity ratio (DCR) at different sections along the pylon computed to establish a damage criterion. The maximum strain in addition to the DCR values are used to evaluate the performance of a proposed octagonal hollow section under blast loads in comparison to the existing rectangular steel sections. In the current study, the DCR is defined as

$$\mathrm{DCR} = \left| \sigma_{\max} / \sigma_y \right|, \tag{1}$$

where $\sigma_{\max}$ is the maximum stress in the section due to design load or blast loads and σ_y is the yield stress. In blast load cases strain rate is taken into account in the calculation of σ_y at each time. A DCR value exceeding unity indicates that the material is in plastic region (material non-linearity).

DESCRIPTION OF MODELS AND ANALYSIS TECHNIQUES

Bridge details

For security reasons, a hypothetical cable stayed steel bridge which is shown in Figure 1 was designed according to minimum requirements of the Australian bridge standard AS5100 (2004) to avoid publishing vulnerabilities for a specific bridge. The proposed bridge consists of three spans, which are 227.5 m, 580 m, and 227.5 m long.

The steel orthotropic box deck is 28 m wide and 2.0 m deep which provides 6 traffic lanes and 2 walkways and designed as a closed hexagon multi-cell box. A 25 mm thick plate was used as top and bottom flange of deck. The longitudinal stiffeners are 400 mm high and spaced at 700 mm for both flanges. Intermediate stiffeners are used for 20 mm web plates at 4 metre spacing. The deck is supported on transverse diaphragms to prevent premature excessive distortional deformation under torsional loading every 10 m. The distance between the diaphragms is reduced to 5 m at both ends of the deck, close to the pylon and at mid-span. A cross-sectional view of the deck is shown in Figure 2. The bridge deck is connected to two A-shaped 136 m tall steel box pylons by 112 cables (Figure 3). A transverse steel box girder connects the pylon legs and the thickness of plates and spacing of the stiffeners inside the pylon box is chosen in such a way that a compact section is provided. The cross-sectional view of the pylon is shown in Figure 4. The cables consist of Grade 270 strands with an ultimate stress of 1860 MPa. The first four cables adjacent to the end supports of the deck are 5 m apart and the other cables are 20 m apart along the bridge deck. The cable area varies from 23,600 mm^2 to 7,700 mm^2 and initial axial post-tensioning varies from 12 MN to 5 MN to provide minimum deflection on deck in respect to permanent loads.

All important components that would have an influence on the bridge response are included such as the diaphragm's stiffeners and manhole. Furthermore, different mesh sizes were used in the FE model to achieve both accuracy and computational efficiency. For example, a finer mesh was used for the zones in the vicinity of the explosion as presented in Figure 5 and Figure 6. The nodes at the base of the pylons are constrained as being fixed in all DOFs while pin support in one end of deck and roller support at the other end were implemented in model.

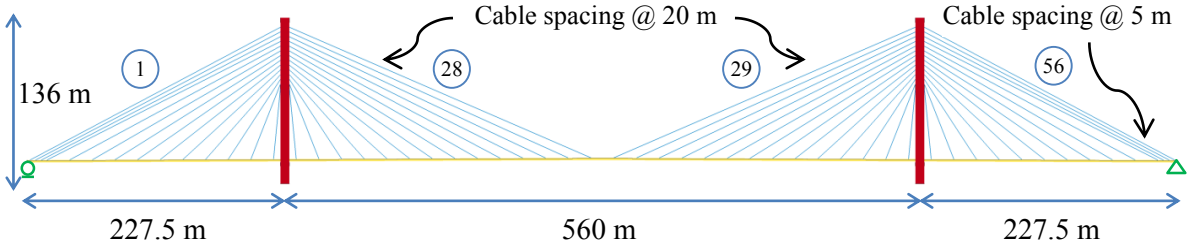

Figure 1 Bridge elevation

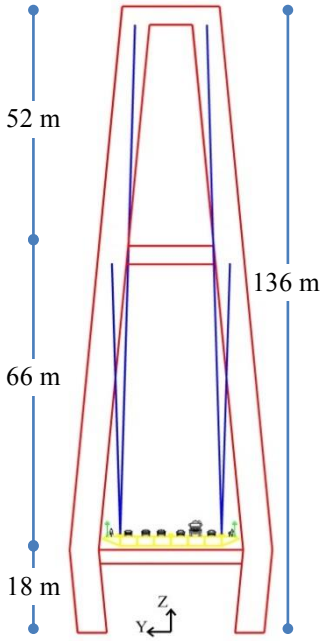

Figure 3 Pylon elevation

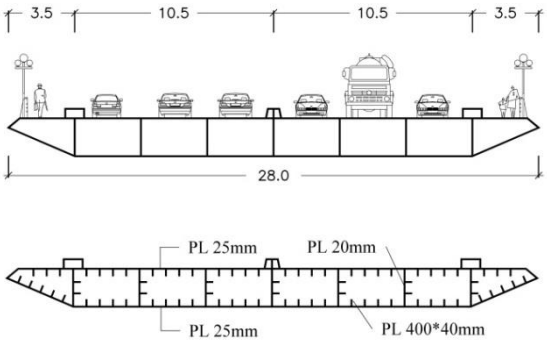

Figure 2 Cross-section of deck

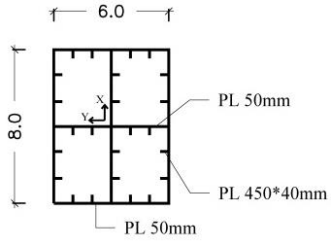

Figure 4 Typical cross-section of pylon

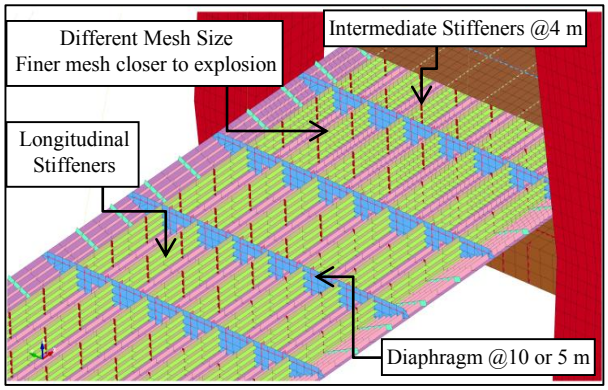

Figure 5 FE model of deck

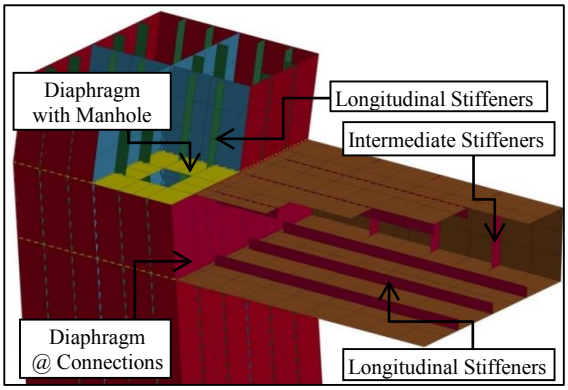

Figure 6 FE model of pylon

Material model and strain rate effects

The steel material used in the deck and pylons is assumed to have elasto-plastic hardening and strain-rate dependency with quadrilateral, fully integrated shell elements. Such an element provides more accurate results and requires a relatively small amount of computation time (Hallquist 2014). The adequacy of material model *MAT_ PIECEWISE_LINEAR_PLASTICITY (MAT_24) in LS-DYNA for modelling the nonlinear behaviour of steel elements subjected to high strain rate loading has been demonstrated through several studies (Jama *et al*. 2009, Hashemi and Bradford 2014). Also, this material model takes advantage of a maximum strain criterion for capturing the onset of failure. The properties of the structural materials are tabulated in Table 1.

Table 1 Material properties

		E	σ_y	σ_u	ε_{max}	A*	I_{yy}*	I_{xx}*	Initial Force
		GPa	MPa	MPa		m^2	m^4	m^4	MN
Deck		200	350	450	0.15	2.735	2.047	194.122	-
Pylon		200	350	450	0.15	2.532	17.431	13.653	-
Cables	Type1	200		1860	0.03	0.0236			12
	Type2	200		1860	0.03	0.0127			9
	Type3	200		1860	0.03	0.0077			5

* The geometrical properties of the pylon cross section were calculated for only one leg.

The yield and ultimate strengths of steel increase under high strain rate while the maximum strain and modulus of elasticity show no specific change to those obtained from static loads. The current study employs the dynamic increase factor to account for the material strength enhancement with strain rate effect for steel, based on the Cowper-Symonds (CS) equation given by

$$\mathrm{DIF_s} = 1 + \left(\dot{\varepsilon}/C\right)^{1/p}, \tag{2}$$

where $\dot{\varepsilon}$ is the strain rate and C and p are Cowper-Symonds constants. For mild steel, Cowper and Symonds (1957) suggested 40.4 s^{-1} and 5 for C and p respectively, while Paik and Thayamballi (2003) suggested values of 3200 s^{-1} and 5 as the CS constants to consider the strain rate on the behaviour of high-strength steel.

The CABLE_DISCRETE_BEAM (MAT_71) material model was used for the elastic cables on the bridge. This material model permits elastic cables to be realistically modelled; thus, no force will develop in compression (Hallquist 2014). The initial post-tensioning forces in cables are given in Table 1. In this study, each component of the bridge structure was given an appropriate material constitutive model.

Gravity and Traffic Loads

The applied loads on the bridge are assumed as gravity load included self-weight (DL) and surfacing (SDL) plus the traffic load (TL), S1600, according to (AS5100 2004). The self-weight is calculated automatically in the software when the keyword *BODY_Z is activated. To consider the connections and weld weight, the deck weight was increased by 15%. 150 mm of insulant and asphalt, as a final coat on the deck, was assumed and applied as a superimposed dead load. Traffic loads were converted to equivalent pressure so they can be easily applied to the shells to minimise the modelling complexity. Two different traffic load cases (TLC) were

considered and denoted TLC1 and TLC2. In TLC1, the traffic loads are assumed to be distributed on the entire bridge deck, while in TLC2, traffic loads are applied only on the main span. Even though both cases were modelled and analysed, only that which gives the severer response is presented herein.

The AASHTO (2012) suggests the load factor for live load γ_{EQ}, shall be determined on a project-specific basis for Extreme Event I and proposed γ_{EQ} = 0.50 is reasonable for a wide range of values of average daily truck traffic in Extreme Event II. Consequently, 50% of the traffic loads (TL) was applied to the model in combination to blast loads.

Blast Scenarios and Explosives weight

Three explosive weights, *viz*. 01W (small), 04W (medium) and 10W (large) were considered in this study. W is the equivalent TNT weight index that is not specified in this study due to security reasons. Four different locations for the explosives were considered to produce the most critical close-range blast loads on pylon (Figure 7). The location of the explosives in the three scenarios was above the deck and in one of the scenarios (*i.e*. BS04), the explosive was placed below the deck and one metre away from the pylon's base. Above the deck explosions were at the possible closest distance to pylon's left leg (BS01), one metre from the middle of the cross-section of the deck at pylon's centre line (BS02) and adjacent to the first cable anchorage zone in the back span (BS03). The following combination of actions is used to evaluate the bridge response under the blast loads (BL):

$$Q = 1.0\times DL+1.4\times SDL+0.5\times TL+1.0\times BL. \quad (3)$$

The *BLAST_ENHANCED command is employed to apply the air blast pressure on the facets defined with the keyword *BLAST_SEGMENT_SET. The normal of each segment should point away from the structure and towards the charge. Additional segments are defined for the bottom flange and the components inside the deck girder to ensure that the extent of damage is captured by the model, in case that the top (surface) flange of the deck is ruptured. In scenario BS04, the combined effect of air blast pressure and ground shock combination have been taken into account.

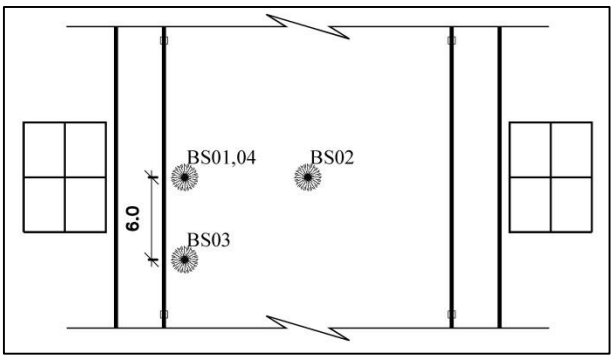

Figure 7 Different blast scenarios (BS)

Blast pressure verification

Before any conclusions regarding the models in this study can be arrived at, the blast modelling and its applied reflected pressure on different parts of the bridge need to be verified. Since a limited amount of experimental data is available in literature, The US Army manuals (UFC-3-340-02 2008) blast pressure prediction which are based on published and unpublished tests, are used to compare the results of finite element analysis herein. For this reason the arrival time and calculated reflected pressures on different elements of the pylon for different explosive weights were obtained and are compared to those in the UFC 3-340-02. Because figure 2-7 in UFC 3-340-02 gives only the normal peak reflected pressures and the normal reflected impulses, only normal values are included in

Figure 8 and

Figure 9. The arrival time is quite similar while the peak reflected pressure is about 15% less than the peak reflected pressure from UFC 3-340-02. According to the verification through the reflected pressure at different points in Figure 9, the calculated blast pressure on the structure is reliable.

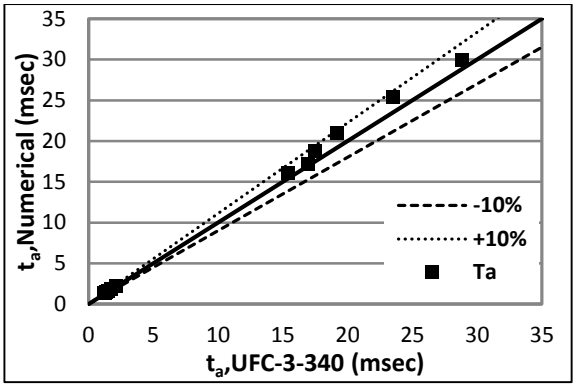

Figure 8 Arrival time

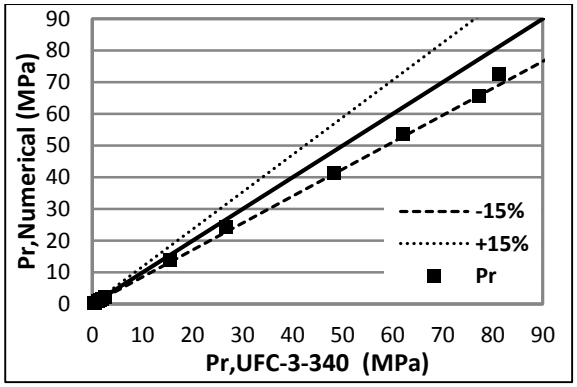

Figure 9 Reflected pressure

RESULTS AND DISCUSSIONS

Dynamic Response of Pylon

When the detonation occurs, the shock front generated from the blast is transferred into the air and travels with high speed until it strikes an object. This causes the wave speed becomes zero and leads to reflected pressure on the object. This reflection is dependent on the geometry, density, blast shock wave speed and arrival time, and other dynamic properties of the object (Son and Lee 2011).

In the scenario with 01W explosive on the deck, the shock causes small localised damage to top flange of the deck, however, no specific deformation is observed at Closer Leg (CL) of the Closer Pylon (CP) to the detonation point. Overall, the bridge remains almost intact under 01W explosive meaning that no repair is required apart from a small area on the deck right under the explosion. No plastic deformation is observed in the structural components and the oscillation of the bridge is damped after a few seconds and the pylons and deck return back to their initial state before the blast. Accordingly, this section focuses more on the bridge response to medium (04W) and large (10W) explosive charges.

The extent of damage in the deck and pylon due to blast loads at different locations above the deck and near the pylon for explosive weights 04W and 10W are shown in Figure 10. The maximum deformation in the pylon for the above the deck explosions occurred in the BS01 scenario, when the explosive is placed in the centre line of the pylon at one side of the deck. The closest face of the pylon to the explosion experienced a large relative deflection as much as 400 mm in 10W detonation which indicates a 12 degree of rotation at the corner support of the plate. Moreover, longitudinal stiffeners and diaphragms attached to that face are affected by the deflection. Moving the position of the explosive along the cross-section (BS02) or along the traffic lanes (BS03) increases the standoff distance as well as the incident angle. The blast pressure in BS03 had minimal impact on the pylon, but its effect on the deck was more critical. According to the FE predictions, in scenario BS03, the cable anchorage zone close to the explosion experienced damage that caused cable detachment even with medium explosive size. In the scenarios BS04-10W, the CP underwent extensive damage. In particular, the explosion caused significant rupture of steel plates in the CP at the level of detonation (Figure 10-h). Crushed zone estimated about 8.5 m height and 8 m wide.

The maximum demand over maximum capacity ratio of the cables connected to the CP on the right hand side (RSeries) and left hand side (LSeries) of the bridge deck along traffic lanes are reported in Figure 11. In scenarios BS01and BS03, the explosives were placed close to the LSeries cables. Since the explosive is not close to the cable anchorage zone in scenario BS01-02, no cable detachment occurs. However, significant increase in the axial force in the cables close to the explosion was observed, and this can potentially lead to their rupture. In those cables close to the pylon, the axial loads increased up to 50 percent more than their capacity under a medium explosion. Under the large explosion, the axial force in the cables reached 2.5 times the axial load capacity of the cables. These results indicate the revision required to recommended DCR values in shorter cables in the case of an explosion on the deck, to produce no cable rupture under medium or large explosion.

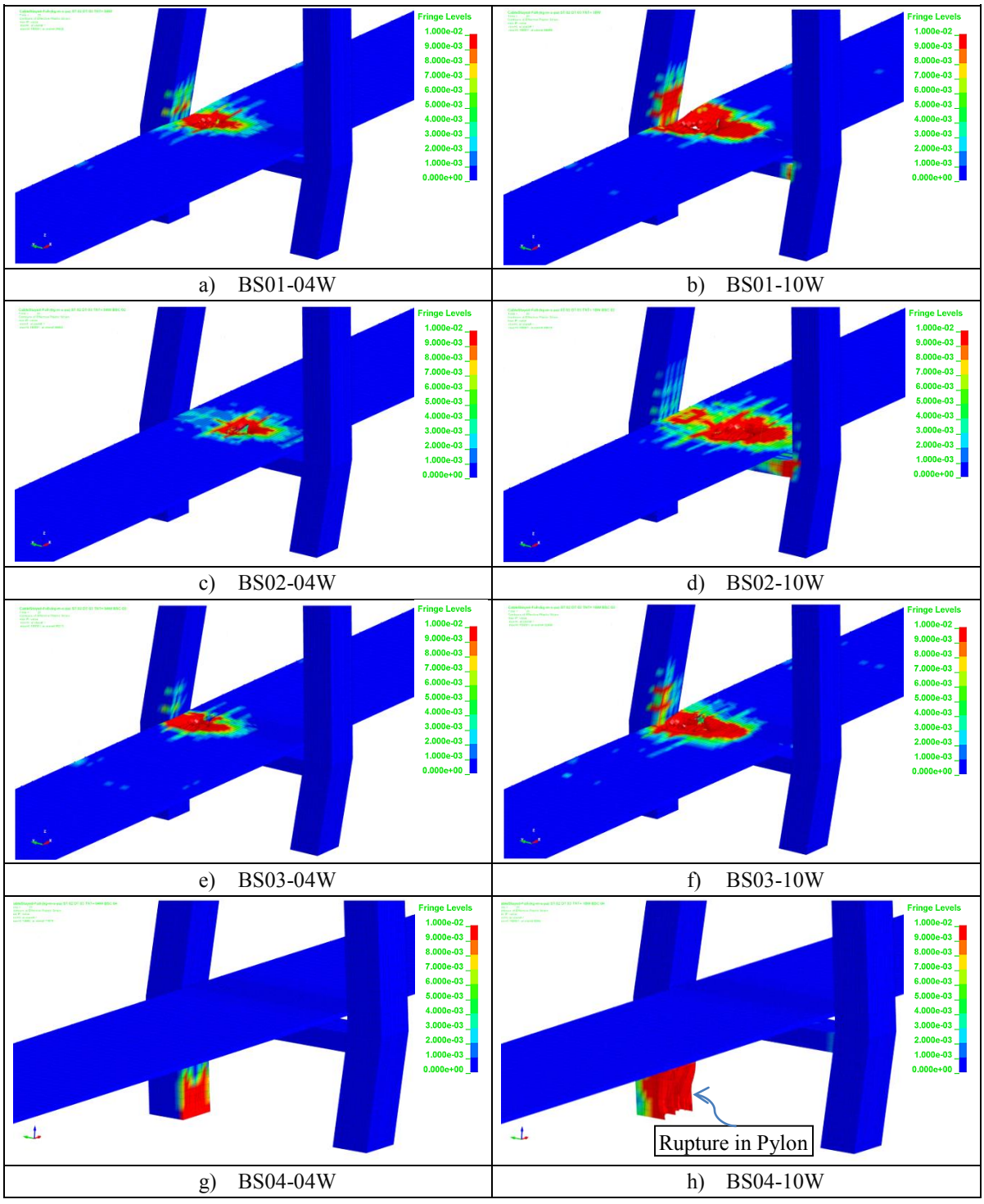

a) BS01-04W b) BS01-10W

c) BS02-04W d) BS02-10W

e) BS03-04W f) BS03-10W

g) BS04-04W h) BS04-10W

Figure 10 Effective plastic strain contours at t = 13 sec.

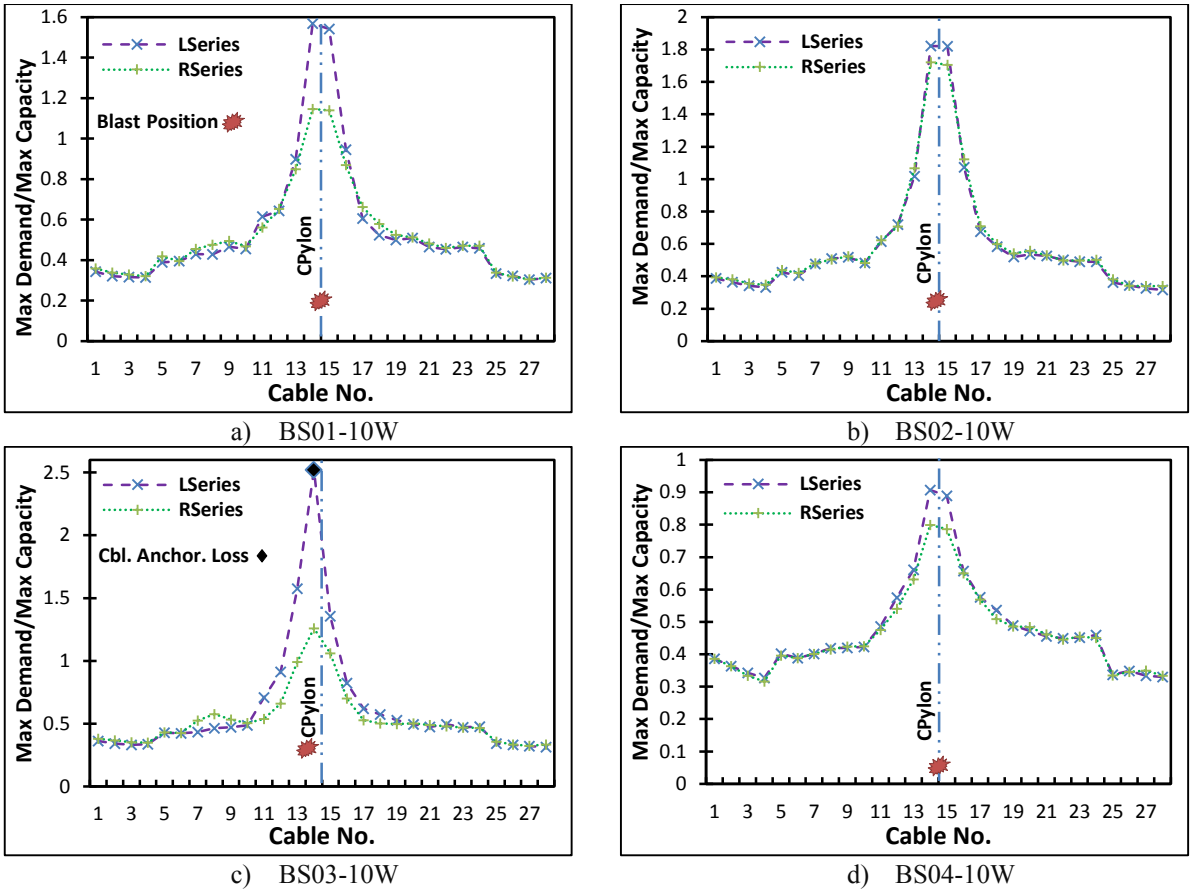

Figure 11 Maximum demand/capacity ratio for cables

DCR results in different blast scenarios

The calculated DCR values under a large explosion at different sections along the pylons are shown in Figure 12 and Figure 13 for different blast scenarios. It should be noted that the results are the maximum response at each section. DCR values and strain reached up to 1.12 and 0.02139 respectively in BS01 and the maximum stress at the explosion level increased to 460 MPa in a 10W explosion. Figure 12 indicates that all blast scenarios have less influence on the Further Pylon (FP). Moreover, because of the large change in cable forces at different BS cases, the upper part of the pylons in which the cable anchorages are placed experience larger blast effects and the DCR values at this location are up to twice the design DCR. In the case in which optimised designed sections are used along the height of a pylon and the design DCR are close to optimum value (say 90%) the change of the demand stress in the section can cause severe blast effects in that part and influence the instability of the pylon.

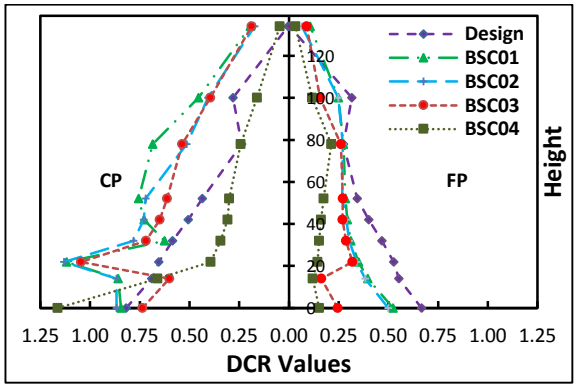

Figure 12 DCR values for CP and FP-10W

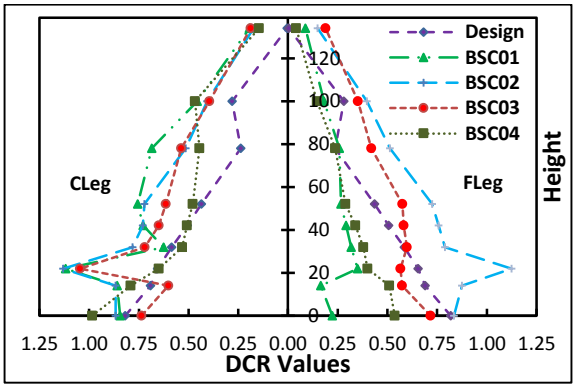

Figure 13 DCR values for CLeg and FLeg-10W

Optimising the pylon section

The variation of the pressure and impulse patterns on the surface of a structure between the maximum and minimum values is a function of the angle of incidence. This angle is formed by the line which defines the normal distance between the point of detonation and the structure, and the line which defines the path of shock propagation between the centre of the explosion and any other point in question on the structure surface (UFC-3-340-02 2008). The maximum reflected pressure and impulse occur when this angle is zero. Changing the angle to 35 degrees will decrease the reflected pressure up to 50% in a larger explosion. Consequently, a circular section with the same area of a rectangular section exposed to an explosion receives less reflected and impulse pressure. Since fabricating a circular section at a very large scale is almost impossible, a modified octagonal section is proposed and shown in Figure 14. This section has almost the same area as the existing rectangular section which means the weight of pylon is the same in both cases. The smaller second moment of area causes more vertical deflection in deck. If the same profile for the deck under self-weight is required, the axial forces in the cables should be adjusted. In this study, it is assumed that cables have the same axial load in new bridge so a new deck profile is achieved in the model.

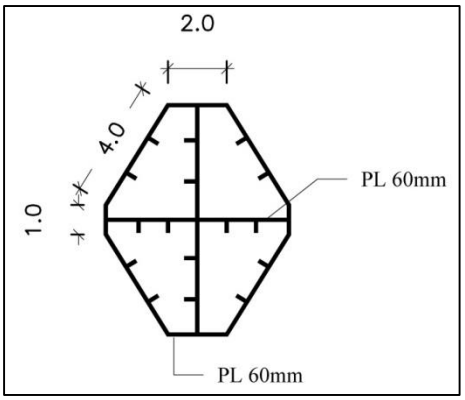

Figure 14 Proposed cross section

The maximum stress in the section at the blast level is the same as the existing section while smaller strain is observed in the section as indicated in Figure 15. The maximum stress and strain occur when the explosive is placed 6 m away from centre line of pylon (BS03). In this scenario, the standoff distance to the pylon is 7.5 m and the maximum angle of incidence is 16 degrees. Placing the explosive closer to the centre of pylon decreases the standoff but increases the angle of incidence, consequently reducing the maximum reflected and impulse pressure on the pylon. For smaller explosions (01-04W), no plastic deflection is observed in the pylon while the maximum DCR and strain value under a large explosion are 1.12 and 0.0088 respectively. Figure 16 shows the comparison of the maximum DCR values between existing rectangular section and proposed octagonal section with different explosive weight.

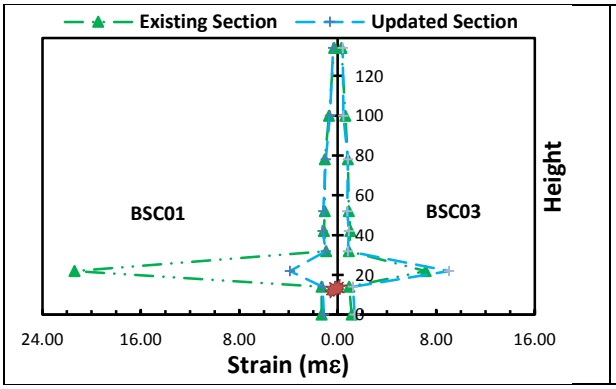

Figure 15 Effective plastic strain -10W

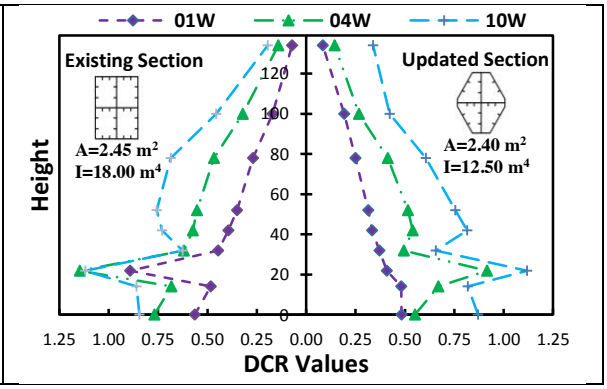

Figure 16 Maximum DCR values at each section

CONCLUSIONS

A detailed model of a hypothetical cable-stayed bridge was produced using LS-DYNA explicit finite element code and the dynamic response of the entire bridge and its components including the pylon, deck and cables were investigated under small to large explosions at different locations close to the pylon. With regard to the local and global responses of the bridge captured by the FE models, the following conclusions are drawn.

- The bridge remained almost intact under a small explosion with no repair required except for a small area in the deck right under the detonation point. However, deck and pylon close to the detonation point underwent plastic strains and rupture in medium and large size explosions. Although extensive damage and steel plate rupture along with large plastic deformations/strains in pylon were observed in some blast scenarios (particularly in large explosions, *i.e*. 10W), the damage did not result in global progressive failure of the pylon in any of the blast scenarios considered in this research. However, the structural components such as the deck and pylons in the vicinity of explosions required major repair and rehabilitation.

- In this study, cable rupture due to axial load exceeding the cable capacity was not considered, but the results of the FE model indicated that shorter cables in the vicinity of the pylon are more vulnerable to the rupture compared to other cables. The FE results also suggest that the revision required to the recommended DCR values in shorter cables in the case of an explosion on the deck to have no cable rupture under medium or large explosion.

- The proposed octagonal hollow section showed better performance under all blast scenarios with different explosive weights. The area of the pylon which is in the plastic region is significantly reduced because of less reflected pressure and impulse on the section due to its geometry. For small and medium explosions, little deflection was observed in the pylon while for a larger explosion a small area in the pylon experienced plastic strains. DCR values are in the same range in different sections whereas the maximum experienced strain is significantly different. Hence, no damage criteria can be stablished based on DCR values individually. The maximum strain in addition to DCR can effectively describe different vulnerabilities.

REFERENCES

AASHTO (2012). *LRFD Bridge Design Specifications*, American Association of State Highway and Transportation Officials.

AS5100 (2004). *Bridge Design*, Standards Australia, Sydney.

Cowper, G. R. Symonds, P.S. (1957). "Strain-hardening and strain-rate effects in the impact loading of cantilever beams". Technical Report 28, Division of Applied Mathematics, Brown University, Providence, RI.

Deng, R.-B. and Jin X.-L. (2009). "Numerical simulation of bridge damage under blast loads". *W. Trans. on Comp*. 8(9), 1564-1574.

FHWA (2003). *Recommendations for Bridge and Tunnel Security*. American Association of State Highway and Transportation Officials,Washington DC.

Hallquist, J. (2014). *LS-DYNA Version 970 Keyword User's Manual*, Livermore Software Technology Corporation (LSTC).

Hao, H. and Tang E. K. C. (2010). "Numerical simulation of a cable-stayed bridge response to blast loads, Part II: Damage prediction and FRP strengthening". *Engineering Structures*, 32(10), 3193-3205.

Hashemi, S. K. and Bradford, M.A. (2014). "The strain-rate effects on the numerical simulation of steel beams under blast loads". *13th International Conference on Structures Under Shock and Impact (SUSI*), New Forest, UK.

Jama, H.H., Bambach, M.R., Nurick, G.N., Grzebieta, R.H. and Zhao, X.-L. (2009). "Numerical modelling of square tubular steel beams subjected to transverse blast loads". *Thin-Walled Structures*, 47(12), 1523-1534.

Paik, J. K. and Thayamballi A. K. (2003). *Ultimate Limit State Design of Steel-Plated Structures*, Wiley, Chichester, UK.

NCHRP (2010). *Blast-Resistant Highway Bridges-Design and Detailing Guidelines (Report 645)*, Transportation Research Board.

Son, J. and Lee, H.J. (2011). "Performance of cable-stayed bridge pylons subjected to blast loading". *Engineering Structures,* 33(4), 1133-1148.

Tang, E.K.C. Hao, H. (2010). "Numerical simulation of a cable-stayed bridge response to blast loads, Part I: Model development and response calculations". *Engineering Structures* 32(10), 3180-3192.

UFC-3-340-02 (2008). *Structures to Resist the Effects of Accidental Explosions*, US Department of Defense, Unified Facilities Criteria (UFC).